

Microporous Organic Network Hollow Spheres: Useful Templates for Nanoparticulate Co_3O_4 Hollow Oxidation Catalysts

Narae Kang,[†] Ji Hoon Park,[†] Mingshi Jin,[†] Nojin Park,[†] Sang Moon Lee,[‡] Hae Jin Kim,[‡] Ji Man Kim,^{*,†} and Seung Uk Son^{*,†}

[†]Department of Chemistry and Department of Energy Science, Sungkyunkwan University, Suwon 440-746, Korea

[‡]Korea Basic Science Institute, Daejeon 350-333, Korea

S Supporting Information

ABSTRACT: Hollow microporous organic networks (H-MONs) were prepared by a template method using silica spheres. The shell thickness was delicately controlled by changing the synthetic conditions. The H-MONs were used as a template for the synthesis of nanoparticulate Co_3O_4 hollows which showed excellent catalytic performance in H_2O_2 oxidation.

Microporous organic networks (MONs) are a new class of functional materials.¹ The MONs have been prepared through various carbon–carbon coupling reactions between organic building blocks.^{1,2} For example, Cooper research group and others have prepared various microporous organic polymers through Sonogashira coupling between alkynes and arylhalides.³ The porosity and functionalities of MONs were controlled by the tailored use of building blocks.^{1–3} The resultant materials have been applied for gas adsorbents and catalysts.^{1–3} In addition to inner porosity, the overall shape of porous materials is also important for their performance. To interact with inner working sites in adsorption or catalysis, guest molecules diffuse into pore structures. The diffusion pathways are dependent on the shape of materials and can be synthetically engineered. As an example of shape effects in material science, hollow spheres showed better efficiencies in electrochemical or photocatalytic performance than nonhollow ones.⁴ In this regard, various hollow structures were designed and prepared.⁵ However, to the best of our knowledge, the shape controlled synthesis of hollow MONs is less explored.⁶

Templated synthesis is a straightforward method for the shape control of materials, because the resultant shapes originating from the sacrificed templates are quite predictable.⁷ For example, silica has been used as a template because it can be removed easily through chemical etching by reaction with HF or NaOH.⁸ Thus, the formation of MON on the surface of silica will be quite an interesting research subject because, if successful, the hollow MONs can be obtained through the chemical etching of silica templates.

In addition to inorganic templates, organic ones have been developed and used for the shape controlled synthesis of inorganic materials.⁹ Because the organic templates can be removed easily through heat-treatment under air, shape-controlled inorganic products can be obtained. If the organic templates have porosity, inorganic precursors can be readily absorbed into the pores to result in the homogeneity of shapes.

Moreover, due to the porosity of templates, particulate walls can be obtained, which can maximize the surface area of materials.

Our research group has studied the synthesis of functional MONs^{6a,10} and the shape controlled synthesis of inorganic nanomaterials,¹¹ separately. In this work, we report the templated synthesis of hollow MON spheres (H-MONs), their successful use as templates for nanoparticulate cobalt oxide hollow spheres, and the excellent catalytic performance as oxidation catalysts.

Figure 1 shows the synthetic scheme for the H-MONs using a silica template. First, monodisperse silica spheres were

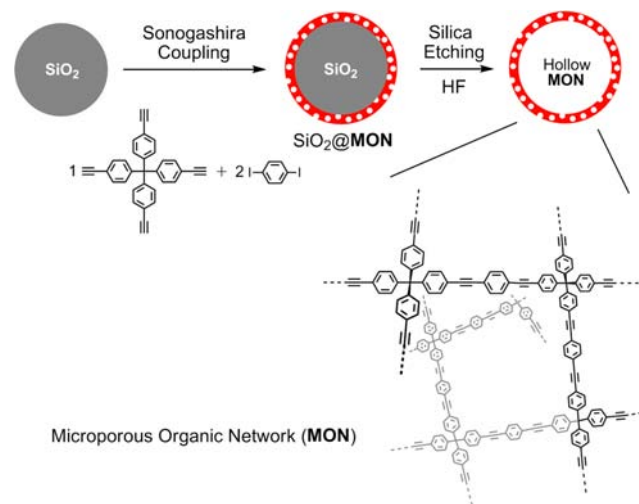


Figure 1. Synthetic route for hollow microporous organic networks (H-MONs) using a silica template.

prepared by Stöber method¹² and well-dispersed in a mixture of toluene and triethylamine. Then, palladium catalyst and copper iodide were added and the reaction mixture was stirred at room temperature for 1 h. Tetra(4-ethynyl)phenylmethane and 2 equiv of 1,4-diodobenzene were added. The reaction mixture was heated at 100 °C for 2 days. The resultant yellow solids were isolated by centrifugation and washed with methylene chloride, acetone and methanol. After drying under vacuum, the materials were treated with HF solution

Received: November 4, 2013

Published: December 9, 2013

for 2 h. The resultant materials were isolated by centrifugation, washed with water, methanol and acetone, and dried under vacuum.

The materials isolated during the synthetic process were investigated by scanning (SEM) and transmission electron microscopy (TEM). The silica templates had a narrow distribution with a 545 ± 17 nm average size (Figure S1). According to TEM studies, the MON shells with a lighter contrast were clearly distinguished from inner darker silica. As shown in Figure 2e, the MON coatings on silica spheres were

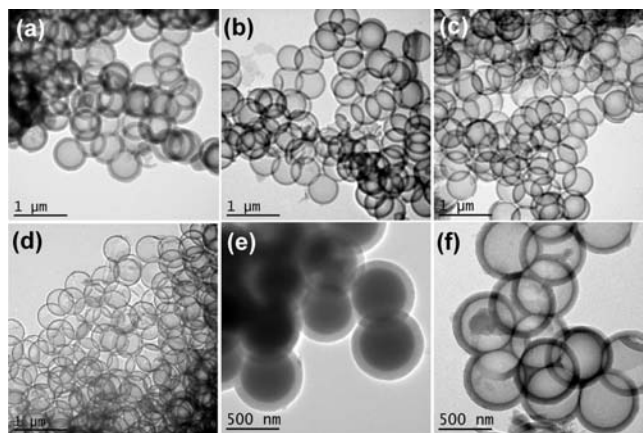


Figure 2. TEM images of hollow MONs (H-MONs) prepared using 50 mg of tetra(4-ethynylphenyl)methane, 80 mg of 1,4-diiodobenzene, 300 mg of silica, and 20 mL/10 mL (a, H-MON-1), 15 mL/15 mL (b, H-MON-2), and 0 mL/30 mL (c, H-MON-3) of toluene/triethylamine. TEM image of H-MON prepared using 50 mg of tetra(4-ethynylphenyl)methane, 80 mg of 1,4-diiodobenzene, 400 mg of silica (d, H-MON-4), and 15 mL/15 mL of toluene/triethylamine. TEM image (e) of silica/MON core/shell materials for H-MON-2. (f) Magnified TEM image of H-MON-2.

quite homogeneous. After the chemical etching of the inner silica with HF, the resultant materials showed a hollow structure (Figure 2f). Through the screening of various synthetic conditions such as solvent and amount of reagents, synthetic methods for thickness control of MON shells were discovered. The four representative synthetic conditions were chosen and the resultant hollow MONs are displayed in Figure 2a–d.

In the case of the solvent system, as the amount of triethylamine increased from 10 mL (H-MON-1) to 15 mL (H-MON-2) and 30 mL (H-MON-3) with a fixed total amount (30 mL) of solvent, the thickness of MON shells gradually decreased from 81 ± 6 to 51 ± 3 and 40 ± 2 nm, respectively (Figures 2a–c and 3a). Also, as expected, when the amount of silica increased from 300 mg (H-MON-2) to 400 mg (H-MON-4), the thickness of shells decreased from 51 ± 3 to 22 ± 2 nm, respectively (Figures 2b,d and 3a). When 500 mg of silica was used with 50 mg of tetra(4-ethynyl)phenylmethane, incomplete hollow structures were dominantly observed (Figure S2).

The analysis of N_2 sorption isotherms based on the Brunauer–Emmett–Teller (BET) theory showed microporosity and high surface areas of the H-MONs in a range of 500–850 m^2/g (Figures 3b, inset, and S3). Interestingly, the surface area of H-MONs decreases gradually from 840 m^2/g (H-MON-1) to 648 m^2/g (H-MON-2) and 572 m^2/g (H-MON-3). When the same amount of triethylamine (15 mL) was used

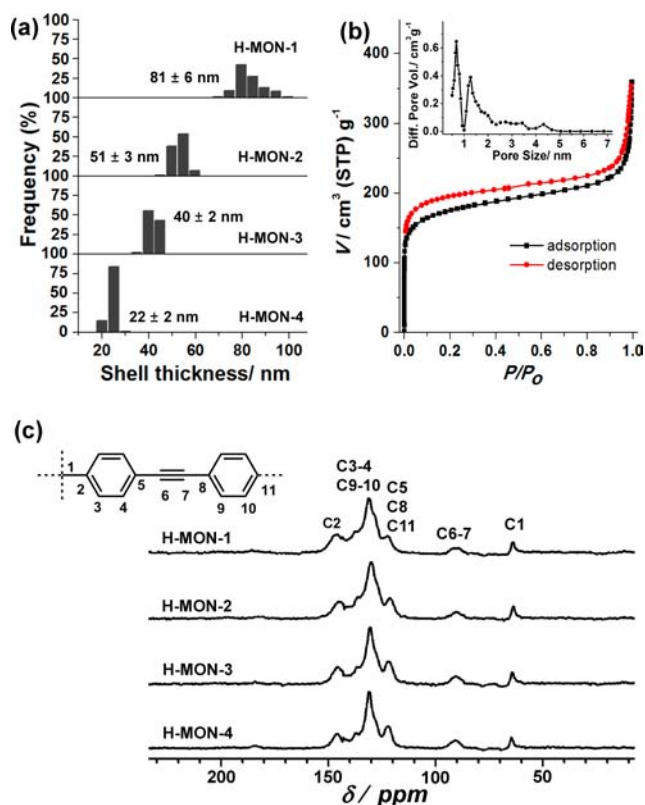


Figure 3. (a) Thickness distribution diagram of H-MON shells. (b) N_2 adsorption/desorption isotherms at 77 K, pore size distribution diagram (DFT method, inset) of H-MON-2. (c) Solid-phase ^{13}C NMR spectra of H-MONs.

with 300 or 400 mg of silica, the surface areas were similar with 648 m^2/g (H-MON-2) and 672 m^2/g (H-MON-4), respectively.¹³ The pore size distribution analysis by density functional theory (DFT) method revealed that the H-MONs have microporosity (<2 nm pores) (Figures 3b, inset, and S3). The solid phase ^{13}C NMR spectra of H-MONs matched well with the expected structure, showing ^{13}C peaks at 90 and 63 ppm from C–C triple bonds and benzylcarbons, respectively (Figure 3c). Thermogravimetric analysis showed that the H-MONs start to decompose at 240–280 °C (Figure S4). Powder X-ray diffraction studies (PXRD) showed an amorphous character of H-MONs, as commonly observed for MONs prepared by Sonogashira coupling in the literature (Figure S5).³

In addition to various application fields reported for nonhollow MONs in the literature,^{1–3} the hollow MONs can be applied for new purposes. In this study, considering the existence of pores in walls, the hollow MONs were applied as an organic template for inorganic hollows (Figure 4a). With an organometallic precursor (cobalt octacarbonyl), cobalt species were introduced into the pores of H-MONs. While we studied the shell thickness effect of H-MON-2 and H-MON-4 as organic templates, the resultant Co_3O_4 hollows showed no significant differences in physical properties such as nanoparticulate shape of walls and surface area (60–67 m^2/g). Thus, we used the H-MON-2 as a representative template. The cobalt oxide/H-MON composites were calcinated at 500 °C for 5 h under air to remove the organic template. The TEM analysis of the hollow cobalt oxides showed the interconnected nanoparticulate structure of walls (Figure 4b,c). High resolution (HR) TEM analysis clearly showed the nanoparticulate

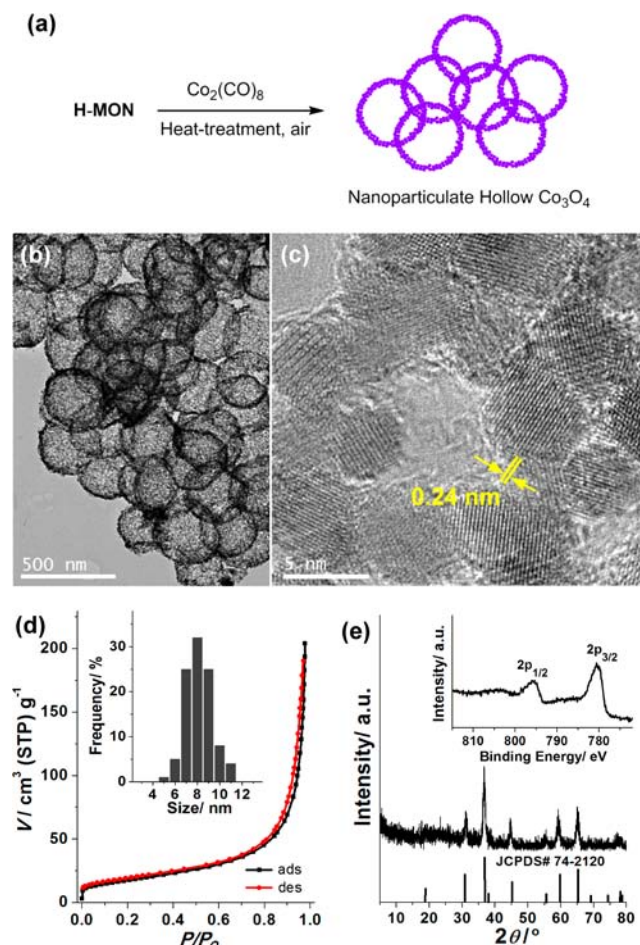


Figure 4. (a) Synthetic scheme, (b) TEM and (c) HR-TEM images, (d) N_2 adsorption/desorption isotherms at 77 K, particle size distribution (inset), (e) PXR pattern and XPS spectrum of Co 2p orbitals of the nanoparticulate Co_3O_4 hollows.

domains and high crystallinity. (Figure 4c). The major (311) crystalline planes with 0.24 nm distance of Co_3O_4 were dominantly observed. According to N_2 sorption isotherm analysis, $64 \text{ m}^2/\text{g}$ of surface area and $0.32 \text{ cm}^3/\text{g}$ pore volume were measured (Figure 4d). The high surface area is attributed to the nanoparticulate walls. The average size of particles in walls was calculated as $7.6 \pm 1.2 \text{ nm}$ by measuring 231 particles (inset Figure 4d). PXR showed that the obtained materials are cubic Co_3O_4 (JCPDS# 74-2120) (Figure 4e). X-ray photoelectron spectroscopy (XPS) showed Co $2p_{3/2}$ orbital peak at 780.3 eV, matching well with the values of Co_3O_4 materials¹⁴ (inset Figure 4e).

Recently, nanostructured cobalt oxides have been applied for environmental oxidation catalysts.^{15,16} For example, cobalt oxides have been applied as oxidation catalysts for the removal of gas pollutants such as CO and NO .¹⁵ In addition, the cobalt oxides have been used for H_2O_2 oxidation for the ultimate removal of organic pollutants in water through the reaction of resultant radical ($\cdot OH$) species.¹⁶ Considering the high surface area of the nanoparticulate Co_3O_4 hollows, we studied their catalytic performance for H_2O_2 oxidation (0.20 M H_2O_2 aqueous solution, 25 mL). Figure 5 summarizes the results. Commercial Co_3O_4 nanoparticles¹⁷ (20 mg) showed 54 mL (89% of theoretical O_2 volume) of oxygen generation for 120 min with $2.4 \times 10^{-2} \text{ min}^{-1}$ rate constant. In comparison, the

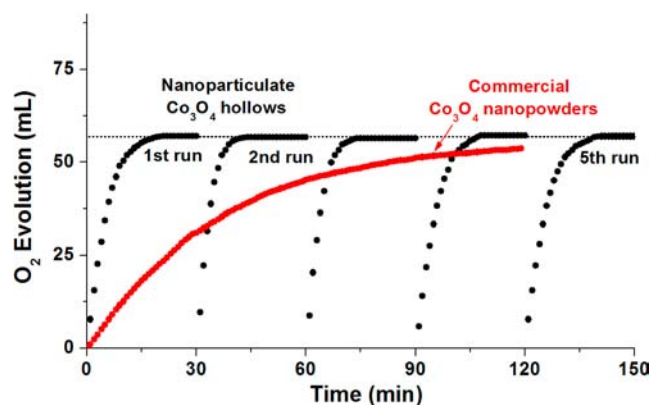


Figure 5. The catalytic performance of the nanoparticulate Co_3O_4 hollows (black line) and commercial Co_3O_4 nanopowders¹⁷ (red line) in H_2O_2 oxidation at 25 °C (20 mg of cobalt catalysts and 25 mL of 0.20 M H_2O_2 aqueous solution were used).

nanoparticulate Co_3O_4 hollows (20 mg) showed 57 mL (93% of theoretical O_2 volume) of oxygen generation within 30 min with $1.8 \times 10^{-1} \text{ min}^{-1}$ rate constant.¹⁸ The recovered Co_3O_4 catalysts retained catalytic activities in the successive runs. Even in the fifth run (57 mL O_2 generation after 30 min, $1.7 \times 10^{-1} \text{ min}^{-1}$ rate constant), there was no significant difference in catalytic activity, compared with that of the first run. The Co_3O_4 hollows recovered after the five runs showed nearly no change in PXR, XPS, and TEM studies (Figure S6). Thus, the use of hollow MONs for the synthesis of nanoparticulate inorganic oxide materials is quite a successful synthetic strategy for the development of new oxidation catalysts.

In conclusion, this work suggests a synthetic method for shape controlled MONs. Using silica templates, monodisperse hollow MONs could be engineered through the chemical etching of a silica template. Moreover, the hollow MON spheres could serve as an organic template for nanoparticulate inorganic hollows. The resultant hollow Co_3O_4 showed excellent catalytic activities in H_2O_2 oxidation. We believe that the hollow MONs in this work can be applied for more diverse purposes including drug delivery. In addition, more diverse inorganic materials can be engineered through screening transition metal sources.

■ ASSOCIATED CONTENT

Supporting Information

Experimental procedure, TEM image of silica templates, additional TEM image for MONs, N_2 adsorption/desorption isotherms, pore size distribution diagrams, TGA curves, and PXR patterns of H-MONs, characterization of the nanoparticulate Co_3O_4 hollow spheres before and after five runs in catalytic H_2O_2 oxidation. This material is available free of charge via the Internet at <http://pubs.acs.org>.

■ AUTHOR INFORMATION

Corresponding Authors

sson@skku.edu
jimankim@skku.edu

Notes

The authors declare no competing financial interest.

■ ACKNOWLEDGMENTS

This work was supported by grants NRF-2012-R1A2A2A01045064 (Midcareer Researcher Program) through NRF of Korea. J.H.P. is grateful for grant 2009-0094023 by the Ministry of Education (Basic Science Research Program).

■ REFERENCES

- (1) Recent reviews on MONs: (a) Dawson, R.; Cooper, A. I.; Adams, D. J. *Prog. Polym. Sci.* **2012**, *37*, 530. (b) Vilela, F.; Zhang, K.; Antonietti, M. *Energy Environ. Sci.* **2012**, *5*, 7919. (c) Thomas, A. *Angew. Chem., Int. Ed.* **2010**, *49*, 8328. (d) Maly, K. E. *J. Mater. Chem.* **2009**, *19*, 1781. (e) Weder, C. *Angew. Chem., Int. Ed.* **2008**, *47*, 448. (f) Mckeown, N. B.; Budd, P. M. *Chem. Soc. Rev.* **2006**, *35*, 675.
- (2) Selected recent examples: (a) McKeown, N. B.; Gahnem, B.; Msayib, K. J.; Budd, P. M.; Tattershall, C. E.; Mahmood, K.; Tan, S.; Book, D.; Langmi, H. W.; Walton, A. *Angew. Chem., Int. Ed.* **2006**, *45*, 1804. (b) Germain, J.; Fréchet, J. M. J.; Svec, F. *J. Mater. Chem.* **2007**, *17*, 7989. (c) Germain, J.; Svec, F.; Fréchet, J. M. J. *Chem. Mater.* **2008**, *20*, 7069. (d) Wood, C. D.; Tan, B.; Trewin, A.; Su, F.; Rosseinsky, M. J.; Bradshaw, D.; Sun, Y.; Zhou, L.; Cooper, A. I. *Adv. Mater.* **2008**, *20*, 1916. (e) Holst, J. R.; Söckel, E.; Adams, D. J.; Cooper, A. I. *Macromolecules* **2010**, *43*, 8531. (f) Bleschke, C.; Schmidt, J.; Kundu, D. S.; Blechert, S.; Thomas, A. *Adv. Synth. Catal.* **2011**, *353*, 3101. (g) Kaur, P.; Hupp, J. T.; Nguyen, S. T. *ACS Catal.* **2011**, *1*, 819. (h) Xie, Z.; Wang, C.; deKrafft, K. E.; Lin, W. *J. Am. Chem. Soc.* **2011**, *133*, 2056. (i) Pandey, P.; Farha, O. K.; Spokoyny, A. M.; Mirkin, C. A.; Kanatzidis, M. G.; Hupp, J. T.; Nguyen, S. T. *J. Mater. Chem.* **2011**, *21*, 1700. (j) Cheng, G.; Hasell, T.; Trewin, A.; Adams, D. J.; Cooper, A. I. *Angew. Chem., Int. Ed.* **2012**, *51*, 12727. (k) Zhang, L. L.; Lin, T.; Pan, X.; Wang, W.; Liu, T.-X. *J. Mater. Chem.* **2012**, *22*, 9861. (l) Zhang, K.; Kopetki, D.; Seeberger, P. H.; Antonietti, M.; Vilela, F. *Angew. Chem., Int. Ed.* **2013**, *52*, 1432. (m) Patel, H. A.; Je, S. H.; Park, J.; Chen, D. P.; Jung, Y.; Yayuz, C. T.; Coskun, A. *Nat. Commun.* **2013**, *4*, 1357. (n) Xu, C.; Hedin, N. *J. Mater. Chem. A* **2013**, *1*, 3406. (o) Zhou, H.; Xu, S.; Su, H.; Wang, M.; Qiao, W.; Ling, L.; Long, D. *Chem. Commun.* **2013**, *49*, 3763. (p) Liang, Q.; Liu, J.; Wei, Y.; Zhao, Z.; MacLachlan, M. J. *Chem. Commun.* **2013**, *49*, 8928.
- (3) (a) Jiang, J.-X.; Su, F.; Trewin, A.; Wood, C. D.; Campbell, N. L.; Niu, H.; Dickinson, C.; Ganin, A. Y.; Rosseinsky, M. J.; Khimyak, Y. Z.; Cooper, A. I. *Angew. Chem., Int. Ed.* **2007**, *46*, 8574. (b) Stöckel, E.; Wu, X.; Trewin, A.; Wood, C. D.; Clowes, R.; Campbell, N. L.; Jones, J. T. A.; Khimyak, Y. Z.; Adams, D. J.; Cooper, A. I. *Chem. Commun.* **2009**, *212*. (c) Jiang, J.-X.; Laybourn, A.; Clowes, R.; Khimyak, Y. Z.; Bacsá, J.; Higgins, S. J.; Adams, D. J.; Cooper, A. I. *Macromolecules* **2010**, *43*, 7577.
- (4) Reviews on the functional hollow materials: (a) Chen, J. S.; Archer, L. A.; Lou, X. W. *J. Mater. Chem.* **2011**, *21*, 9912. (b) Mahmoud, M. A.; Narayanan, R.; El-Sayed, M. A. *Acc. Chem. Res.* **2013**, *46*, 1795.
- (5) Selected recent examples: (a) Yin, Y.; Erdonmez, C.; Aloni, S.; Alivisatos, A. P. *J. Am. Chem. Soc.* **2006**, *128*, 12671. (b) Peng, S.; Sun, S. *Angew. Chem., Int. Ed.* **2007**, *46*, 4155. (c) Xu, H.; Wang, W. *Angew. Chem., Int. Ed.* **2007**, *46*, 1489. (d) Wang, J.; Yang, N.; Tang, H.; Dong, Z.; Jin, Q.; Yang, M.; Kisailus, D.; Zhao, H.; Tang, Z.; Wang, D. *Angew. Chem., Int. Ed.* **2013**, *52*, 6417. (e) Böttger-Hiller, F.; Kempe, P.; Cox, G.; Panchenko, A.; Janssen, N.; Petzold, A.; Thurn-Albrecht, T.; Borchardt, L.; Rose, M.; Kaskel, S.; Georgi, C.; Lang, H.; Spange, S. *Angew. Chem., Int. Ed.* **2013**, *52*, 6088.
- (6) (a) Chun, J.; Park, J. H.; Kim, J.; Lee, S. M.; Kim, H. J.; Son, S. U. *Chem. Mater.* **2012**, *24*, 3458. (b) Li, B.; Yang, X.; Xia, L.; Majeed, M. I.; Tan, B. *Sci. Rep.* **2013**, *3*, 2128.
- (7) Recent review: Liu, Y.; Goebel, J.; Yin, Y. *Chem. Soc. Rev.* **2013**, *42*, 2610.
- (8) Selected examples: (a) Xu, X.; Asher, S. A. *J. Am. Chem. Soc.* **2004**, *126*, 7940. (b) Arnal, P. M.; Comotti, M.; Schüth, F. *Angew. Chem., Int. Ed.* **2006**, *45*, 8224.
- (9) Selected examples: (a) Agrawal, M.; Gupta, S.; Pich, A.; Zafeiropoulos, N. E.; Stamm, M. *Chem. Mater.* **2009**, *21*, 5343.
- (b) Sanlés-Sobrido, M.; Pérez-Lorenzo, M.; Rodríguez-González, B.; Salgueirino, V.; Correa-Duarte, M. A. *Angew. Chem., Int. Ed.* **2012**, *51*, 3877. (c) Sasidharan, M.; Zenibana, H.; Nandi, M.; Bhaumik, A.; Nakashima, K. *Dalton Trans.* **2013**, *42*, 13381.
- (10) (a) Cho, H. C.; Lee, H. S.; Chun, J.; Lee, S. M.; Kim, H. J.; Son, S. U. *Chem. Commun.* **2011**, *47*, 917. (b) Lee, H. S.; Choi, J.; Jin, J.; Chun, J.; Lee, S. M.; Kim, H. J.; Son, S. U. *Chem. Commun.* **2012**, *48*, 94. (c) Kang, N.; Park, J. H.; Choi, J.; Jin, J.; Chun, J.; Jung, I. G.; Jeong, J.; Park, J.-G.; Lee, S. M.; Kim, H. J.; Son, S. U. *Angew. Chem., Int. Ed.* **2012**, *51*, 6626. (d) Kang, N.; Park, J. H.; Ko, K. C.; Chun, J.; Kim, E.; Shin, H. W.; Lee, S. M.; Kim, H. J.; Ahn, T. K.; Lee, J. Y.; Son, S. U. *Angew. Chem., Int. Ed.* **2013**, *52*, 6228. (e) Chun, J.; Kang, S.; Kang, N.; Lee, S. M.; Kim, H. J.; Son, S. U. *J. Mater. Chem. A* **2013**, *1*, 5517.
- (11) (a) Park, K. H.; Jang, K.; Son, S. U. *Angew. Chem., Int. Ed.* **2006**, *45*, 4608. (b) Park, K. H.; Jang, K.; Kim, S.; Kim, H. J.; Son, S. U. *J. Am. Chem. Soc.* **2006**, *128*, 14780. (c) Park, K. H.; Jang, K.; Son, S. U. *Angew. Chem., Int. Ed.* **2007**, *46*, 1152. (d) Park, K. H.; Choi, J.; Kim, H. J.; Oh, D.-H.; Ahn, J. R.; Son, S. U. *Small* **2008**, *4*, 945. (e) Xu, J.; Jang, K.; Jung, I. G.; Kim, H. J.; Oh, D.-H.; Ahn, J. R.; Son, S. U. *Chem. Mater.* **2009**, *21*, 4347. (f) Choi, J.; Kang, N.; Yang, H. Y.; Kim, H. J.; Son, S. U. *Chem. Mater.* **2010**, *22*, 3586. (g) Choi, J.; Jin, J.; Jung, I. G.; Kim, J. M.; Kim, H. J.; Son, S. U. *Chem. Commun.* **2011**, *47*, 5241. (h) Choi, J.; Jin, J.; Lee, J.; Park, J. H.; Kim, H. J.; Oh, D.-H.; Ahn, J. R.; Son, S. U. *J. Mater. Chem.* **2012**, *22*, 11107. (i) Xu, J.; Jin, J.; Kim, K.; Shin, Y. J.; Kim, H. J.; Son, S. U. *Chem. Commun.* **2013**, *49*, 5981.
- (12) Stöber, W.; Fink, A.; Bohn, E. *J. Colloid Interface Sci.* **1968**, *26*, 62.
- (13) Unfortunately, underlying reasons are not clarified yet.
- (14) Moulder, J. F.; Stickle, W. F.; Sobol, P. E.; Bomben, K. D. *Handbook of X-ray Photoelectron Spectroscopy*; Chastain, J., King, R. C., Jr., Eds.; Physical Electronics Inc.: Eden Prairie, MN, 1992.
- (15) Selected examples: (a) Xie, X.; Li, Y.; Liu, Z.-Q.; Haruta, M.; Shen, W. *Nature* **2009**, *458*, 746. (b) Irfan, M. F.; Goo, J. H.; Kim, S. D. *Appl. Catal. B* **2008**, *78*, 267. (c) Sun, Y.; Lv, P.; Yang, J.-Y.; He, L.; Nie, J.-C.; Liu, X.; Li, Y. *Chem. Commun.* **2011**, *47*, 11279. (d) Yan, N.; Chen, Q.; Wang, F.; Wang, Y.; Zhong, H.; Hu, L. *J. Mater. Chem. A* **2013**, *1*, 637.
- (16) (a) Jin, M.; Park, J.-N.; Shon, J. K.; Li, Z.; Lee, E.; Kim, J. M. *J. Porous Mater.* **2013**, *20*, 989. (b) Makhlof, M. T.; Abu-Zied, B. M.; Mansoure, T. H. *Appl. Sur. Sci.* **2013**, *274*, 43.
- (17) Co₃O₄ nanopowder (<50 nm, Aldrich Co., Cat. No. 637025) was used.
- (18) Recently, the mesoporous Co₃O₄ showing 1.1 × 10⁻¹ min⁻¹ rate constant at 25 °C was reported (ref 16a).